NASA Contractor Report 165986

THREE-DIMENSIONAL ELASTICITY SOLUTION OF AN INFINITE PLATE WITH A CIRCULAR HOLE

F. Delale and F. Erdogan

LEHIGH UNIVERSITY
Bethlehem, Pennsylvania 18015

Grant NGR 39-007-011
September 1982

National Aeronautics and
Space Administration

Langley Research Center
Hampton, Virginia 23665

THREE-DIMENSIONAL ELASTICITY SOLUTION OF AN INFINITE PLATE WITH A CIRCULAR HOLE

BY
F. Delale* and F. Erdogan
Lehigh University, Bethlehem PA

Abstract

In this paper the elasticity problem for a thick plate with a circular hole is formulated in a systematic fashion by using the z-component of the Galerkin vector and that of Muki's harmonic vector function. The problem was originally solved by Alblas [1]. The reasons for reconsidering it are to develop a technique which may be used in solving the elasticity problem for a multilayered plate and to verify and extend the results given by Alblas. As in [1] the problem is reduced to an infinite system of algebraic equations which is solved by the method of reduction. Various stress components are tabulated as functions of a/h, z/h, r/a, and ν, a and 2h being the radius of the hole and the plate thickness and ν the Poisson's ratio. Among the additonal results of particular interest one may mention the significant effect of the Poisson's ratio on the behavior and the magnitude of the stresses.

1. Introduction

In this paper the three-dimensional elasticity problem of a thick plate containing a circular hole and subjected to unidirectional loading away from the hole region is reconsidered. The problem was originally solved by Alblas for stretching as well as bending of the plate [1]. Alblas obtained the elasticity solution of the problem by formulating it in terms of three displacement potentials and by reducing it to an infinite system of linear algebraic equations. Basically this system of equations arises from the expansion of the boundary conditions on the hole surface into series of complex eigenfunctions. The infinite system was then solved by the method of reduction and the results were compared with varous existing approximate solutions.

The main reason for reconsidering the problem in this paper is to develop a technique for thick plates which may be used in a straight-

*After September 1981, Department of Mechanical Engineering and Mechanics, Drexel University, Philadelphia PA

forward manner for solving the elasticity problem of a multilayered plate containing a circular hole. The practical importance of the latter problem lies in the fact that under unidirectional compressive loading of the layered medium the transverse normal stress σ_{zz} on the interface is tensile around the hole where there is a stress concentration in $\sigma_{\theta\theta}$ and, in fact, has a (weak) power singularity at the hole boundary which greatly enhances the possibility of delamination failure. In this study the thick plate problem is formulated in a systematic manner by using the z-component of the Galerkin vector and that of a harmonic vector function introduced by Muki [2]. By using a complex eigenfunction expansion for the tractions on the hole boundary this formulation also leads to an infinite system of algebraic equations. The z-component of Muki's vector function turns out to be identical to the displacement potential A used by Alblas, the z-component of the Galerkin vector is biharmonic, and it appears that the potentials A, B_1, and B_2 of [1] constitute a special case of the functions ψ and Z used in this paper. In fact the characteristic equation giving the eigenvalues obtained in this paper is identical to that found in [1].

In the numerical results presented in [1] seven eigenvalues were computed and in the series expansion at most seven terms were considered. Thus, a secondary reason for reconsidering the problem is to verify and to complement the results given in [1] by using greater number of terms in the series and by providing additional results. For example, in [1] the results are given for ν=0.25 only whereas in the perturbation problem the Poisson's ratio turns out to have a very significant effect on the nature as well as on the magnitude of the stresses.

The problem of thick plate containing a circular hole has recently been studied also by Aguf and Vasil´ev [3] under general axisymmetric boundary conditions on the plate surfaces. In [3] even though the general problem was also reduced to an infinite system of algebraic equations, the results given in the paper for a plate loaded symmetrically with respect to midplane of the plate were obtained essentially by a two-step successive approximations, each step involving the solution of a somewhat standard axisymmetric contact problem. In literature there are also a number of approximate solutions of the problem reviews of which may be found in [1-3]

(see, for example [4]).

2. Formulation and Solution

Consider an infinite plate of thickness 2h subjected to unidirectional stress $\sigma_{xx} = \sigma_o$ at $x = \pm \infty$ (Figure 1). In cylindrical coordinates the stress state in the plate without a hole may be expressed as

$$\sigma_{rr} = \frac{\sigma_o}{2}(1 + \cos 2\theta) \quad , \quad \sigma_{\theta\theta} = \frac{\sigma_o}{2}(1 - \cos 2\theta) \quad ; \quad \sigma_{zz} = 0 \quad ,$$
$$\sigma_{r\theta} = -\frac{\sigma_o}{2}\sin 2\theta \quad , \quad \sigma_{rz} = 0 \quad , \quad \sigma_{\theta z} = 0 \quad . \tag{1a-f}$$

To solve the problem of a plate having a traction-free circular hole of radius a the perturbation solution of the plate obtained by using the following boundary conditions must be added to that given by (1)

$$\sigma_{rr}(a,\theta,z) = -\frac{\sigma_o}{2}(1 + \cos 2\theta) \quad , \quad \sigma_{r\theta}(a,\theta,z) = \frac{\sigma_o}{2}\sin 2\theta \quad ,$$
$$\sigma_{rz}(a,\theta,z) = 0 \quad ; \quad (\sigma_{rr}, \sigma_{r\theta}, \sigma_{rz}) \to 0, \text{ as } r \to \infty \quad . \tag{2a-d}$$

The superposition of θ-independent solutions given by (1) and that obtained from (2) gives the axisymmetric solution of a thick plate containing a traction-free circular hole and subjected to a uniform radial stress $\sigma_{rr} = \sigma_o/2$ at $r = \infty$. This solution is known to be independent of z and is given by [1]

$$\sigma^a_{rr} = \frac{\sigma_o}{2}\left(1 - \frac{a^2}{r^2}\right) \quad , \quad \sigma^a_{\theta\theta} = \frac{\sigma_o}{2}\left(1 + \frac{a^2}{r^2}\right) \quad , \quad \sigma^a_{r\theta} = 0 \quad ,$$
$$\sigma^a_{rz} = 0 \quad , \quad \sigma^a_{\theta z} = 0 \quad , \quad \sigma^a_{zz} = 0 \quad , \quad (a \le r < \infty \ , \ |z| \le h \ , \ 0 \le \theta \le 2\pi) \ . \tag{3}$$

Thus, the problem under consideration is reduced to a perturbation problem having the following boundary conditions:

$$\sigma^b_{rr}(a,\theta,z) = -\frac{\sigma_o}{2}\cos 2\theta \quad , \quad \sigma^b_{r\theta}(a,\theta,z) = \frac{\sigma_o}{2}\sin 2\theta \quad ,$$
$$\sigma^b_{rz}(a,\theta,z) = 0 \quad ; \quad (\sigma^b_{rr}, \sigma^b_{r\theta}, \sigma^b_{rz}) \to 0 \quad , \quad \text{as } r \to \infty \quad . \tag{4a-d}$$

The complete solution of the problem of a unidirectionally loaded thick

plate with a traction-free circular hole may then be expressed as

$$\sigma_{ij}(r,\theta,z) = \sigma^{a}_{ij}(r) + \sigma^{b}_{ij}(r,\theta,z) + \sigma^{c}_{ij}(\theta) \quad , \quad (i,j = r,\theta,z), \tag{5}$$

where, referring to (1)

$$\sigma^{c}_{rr}(\theta) = \frac{\sigma_o}{2}\cos 2\theta \quad , \quad \sigma^{c}_{\theta\theta}(\theta) = -\frac{\sigma_o}{2}\cos 2\theta,$$
$$\sigma^{c}_{r\theta} = -\frac{\sigma_o}{2}\sin 2\theta \quad , \quad \sigma^{c}_{zz} = \sigma^{c}_{rz} = \sigma^{c}_{\theta z} = 0 \quad . \tag{6}$$

The geometry of the medium and the boundary conditions suggest that the stress state $\sigma^{b}_{ij}(r,\theta,z)$, $(i,j = r,\theta, z)$ for the perturbation problem will have the following form:

$$\sigma^{b}_{rr} = \tau_{rr}(r,z)\cos 2\theta \quad , \quad \sigma^{b}_{\theta\theta} = \tau_{\theta\theta}(r,z)\cos 2\theta \quad ,$$
$$\sigma^{b}_{r\theta} = \tau_{r\theta}(r,z)\sin 2\theta \quad , \quad \sigma^{b}_{rz} = \tau_{rz}(r,z)\cos 2\theta \quad , \tag{7a-f}$$
$$\sigma^{b}_{\theta z} = \tau_{\theta z}(r,z)\sin 2\theta \quad , \quad \sigma^{b}_{zz} = \tau_{zz}(r,z)\cos 2\theta \quad .$$

Let $Z(r,\theta,z)$ and $\psi(r,\theta,z)$ respectively be the z-component of the Galerkin vector and that of the harmonic vector function introduced by Muki [2]. The functions Z and ψ satisfy the following differential equations:

$$\nabla^2\nabla^2 Z = 0 \tag{8}$$

$$\nabla^2\psi = 0 \quad , \quad \nabla^2 = \frac{\partial^2}{\partial r^2} + \frac{\partial}{r\partial r} + \frac{\partial^2}{r^2\partial\theta^2} + \frac{\partial^2}{\partial z^2} \tag{9}$$

The form of the stress state as given by (7) and the relationship between the stresses and the functions Z and ψ imply that these functions may be expressed as [2]

$$Z(r,\theta,z) = Z_1(r,z)\cos 2\theta \tag{10}$$

$$\psi(r,\theta,z) = \psi_1(r,z)\sin 2\theta \tag{11}$$

From (8-11) it follows that

$$\nabla_2^2 \nabla_2^2 Z_1 = 0 \quad , \tag{12}$$

$$\nabla_2^2 \psi_1 = 0 \quad , \quad \nabla_2^2 = \frac{\partial^2}{\partial r^2} + \frac{\partial}{r\partial r} - \frac{4}{r^2} + \frac{\partial^2}{\partial z^2} \quad . \tag{13}$$

The functions Z_1 and ψ_1 defined by (10) and (11) satisfy the following symmetry relations:

$$Z_1(r,z) = - Z_1(r,-z) \quad , \quad \psi_1(r,z) = \psi_1(r,-z) \quad . \tag{14a,b}$$

Let us now assume that Z_1 and ψ_1 are given by

$$\psi_1(r,z) = \sum_1^\infty f_k(r) \cos \beta_k z \quad , \tag{15}$$

$$Z_1(r,z) = \sum_1^\infty g_n(r) \sin \alpha_n z + \sum_1^\infty h_n(r)\, z \cos \alpha_n z. \tag{16}$$

Substituting from (15) and (16) into (13) and (12) we obtain

$$f_k(r) = A_k K_2(\beta_k r) + A_k^* I_2(\beta_k r) \quad , \tag{17}$$

$$\begin{aligned} g_n(r) = {} & B_n K_2(\alpha_n r) + D_n \alpha_n r K_3(\alpha_n r) \\ & + B_n^* I_2(\alpha_n r) + D_n^* \alpha_n r I_3(\alpha_n r) \quad , \end{aligned} \tag{18}$$

$$h_n(r) = C_n K_2(\alpha_n r) + C_n^* I_2(\alpha_n r) \quad . \tag{19}$$

From (15-19) and the regularity conditions (4d) at $r = \infty$ it follows that

$$A_k^* = 0,\ B_k^* = 0,\ D_k^* = 0,\ C_k^* = 0, \ (k = 1,2, \ldots) \tag{20}$$

Also, it can be shown that the boundary condition $\sigma_{zz}^b(r,\theta,\pm h) = 0$ or $\tau_{rz}(r,\pm h) = 0$ may be expressed in the following form:

$$F_1(B_n, C_n, D_n)\, F_2(r) + D_n F_3(r) = 0 \quad , \ (a<r<\infty) \quad , \tag{21}$$

where F_1, F_2, and F_3 are known functions. Thus for (21) to be valid for all r in (a,∞) one must have

$$F_1(B_n, C_n, D_n) = 0 \quad , \quad D_n = 0 \quad . \tag{22a,b}$$

By considering (20) and (22b) the functions ψ_1 and Z_1 may be expressed as

$$\psi_1(r,z) = \sum_{k=1}^{\infty} A_k K_2(\beta_k r) \cos \beta_k z \quad , \tag{23}$$

$$Z_1(r,z) = \sum_{n=1}^{\infty} [B_n K_2(\alpha_n r) \sin \alpha_n z + C_n K_2(\alpha_n r) z \cos \alpha_n z]. \tag{24}$$

The three sets of constants A_n, B_n, and C_n, (n = 1,2, ...) and the "eigenvalues" α_n and β_n, (n = 1,2, ...) may be obtained from the boundary conditions at r = a and z ± h. Referring to (7) the conditions at z = ± h may be expressed as

$$\tau_{zz}(r, \pm h) = 0 \quad , \quad \tau_{rz}(r, \pm h) = 0 \quad , \quad \tau_{\theta z}(r, \pm h) = 0, (a<r<\infty) \tag{25}$$

In terms of the functions Z and ψ the stresses in the plate are given by

$$\sigma^b_{rr} = \frac{\partial}{\partial z}(\nu\nabla^2 - \frac{\partial^2}{\partial r^2}) Z + \frac{\partial}{\partial \theta}(\frac{2}{r}\frac{\partial}{\partial r} - \frac{2}{r^2})\psi \quad ,$$

$$\sigma^b_{r\theta} = \frac{1}{r}\frac{\partial^2}{\partial \theta \partial z}(\frac{1}{r} - \frac{\partial}{\partial r})Z - (2\frac{\partial^2}{\partial r^2} + \frac{\partial^2}{\partial z^2})\psi \quad ,$$

$$\sigma^b_{\theta\theta} = \frac{\partial}{\partial z}(\nu\nabla^2 - \frac{1}{r}\frac{\partial}{\partial r} - \frac{1}{r^2}\frac{\partial^2}{\partial \theta^2})Z - \frac{\partial}{\partial \theta}(\frac{2}{r}\frac{\partial}{\partial r} - \frac{2}{r^2})\psi \quad , \tag{26a-f}$$

$$\sigma^b_{zz} = \frac{\partial}{\partial z}[(2-\nu)\nabla^2 - \frac{\partial^2}{\partial z^2}]Z \quad ,$$

$$\sigma^b_{rz} = \frac{\partial}{\partial r}[(1-\nu)\nabla^2 - \frac{\partial^2}{\partial z^2}]Z + \frac{1}{r}\frac{\partial^2 \psi}{\partial \theta \partial z} \quad ,$$

$$\sigma^b_{\theta z} = \frac{1}{r}\frac{\partial}{\partial \theta}[(1-\nu)\nabla^2 - \frac{\partial^2}{\partial z^2}]Z - \frac{\partial^2 \psi}{\partial \theta \partial z} \quad .$$

Now by substituting from (7), (10), (11), (23) and (24) into (26d-f) we obtain

$$\tau_{zz}(r,z) = \sum_{1}^{\infty} \alpha_n^2 K_2(\alpha_n r)\{(\alpha_n \cos \alpha_n z)B_n - [(1-2\nu)\cos \alpha_n z + \alpha_n z \sin \alpha_n z]C_n\} \quad ,$$

$$\tau_{rz}(r,z) = \sum_{n=1}^{\infty} \alpha_n K_2'(\alpha_n r)\{(\alpha_n \sin \alpha_n z)B_n + (2\nu \sin \alpha_n z + \alpha_n z \cos \alpha_n z)C_n\} - \frac{2}{r}\sum_{k=1}^{\infty} A_k \beta_k K_2(\beta_k r) \sin \beta_k z \quad , \tag{27a-c}$$

$$\tau_{\theta z}(r,z) = -\frac{2}{r}\sum_{n=1}^{\infty} \alpha_n K_2(\alpha_n r)[(\alpha_n \sin \alpha_n z)B_n + (2\nu \sin \alpha_n z$$

$$+ \alpha_n z \cos \alpha_n z)C_n] + \sum_{k=1}^{\infty} A_k \beta_k K_2'(\beta_k r) \sin \beta_k z.$$

From (25) and (27) it then follows that

$$\sin \beta_k h = 0 \quad , \quad \beta_k = \pi k/h \quad , \tag{28}$$

$$(\alpha_n \cos \alpha_n h)B_n - [(1-2\nu) \cos \alpha_n h + \alpha_n h \sin \alpha_n h]C_n = 0 \quad ,$$

$$(\alpha_n \sin \alpha_n h)B_n + [2\nu \sin \alpha_n h + \alpha_n h \cos \alpha_n h]C_n = 0 \quad . \tag{29a,b}$$

For a non zero solution the determinant of the coefficients in (29) must vanish giving the following characteristic equation for α_n:

$$2\lambda_n + \sin 2\lambda_n = 0 \quad , \quad \lambda_n = \alpha_n h \quad , \quad (n = 1,2, \ldots) \quad . \tag{30}$$

From (30) it is seen that if λ_n is a root $-\lambda_n$, $\bar{\lambda}_n$, and $-\bar{\lambda}_n$ are also roots. Therefore, it is sufficient to determine the roots of (30) in the first quadrant of the λ plane only. Also, from (29) we have

$$B_n = \left(\frac{1-2\nu}{\lambda_n} + \tan \lambda_n\right)hC_n \quad . \tag{31}$$

Let us now define the following dimensionless quantities:

$$A_k' = A_k/(ah\sigma_o) \quad , \quad C_n' = C_n/(ah\sigma_o) \quad ,$$

$$s = z/h \quad , \quad \rho = r/a \quad , \quad t = a/h \quad . \tag{32}$$

The stress coefficients τ_{ij} defined by (7) and generated by the functions Z_1 and ψ_1 may then be expressed as follows:

$$\frac{\tau_{zz}(\rho,s)}{\sigma_o} = \mathrm{Re} \sum_{n=1}^{\infty} C_n' [\lambda_n^3 t K_2(\lambda_n \rho t)(\tan \lambda_n \cos \lambda_n s - s \sin \lambda_n s)]$$

$$\frac{\tau_{rz}(\rho,s)}{\sigma_o} = - R_e \sum_{n=1}^{\infty} C_n' [\lambda_n t K_1(\lambda_n \rho t) + \frac{2}{\rho} K_2(\lambda_n \rho t)]^*$$

$$*[\lambda_n \sin \lambda_n s + \lambda_n^2 \tan \lambda_n \sin \lambda_n s + \lambda_n^2 s \cos \lambda_n s]$$

$$- \frac{2}{\rho} \sum_{k=1}^{\infty} A_k' k\pi K_2(k\pi\rho t) \sin k\pi s \quad ,$$

$$\frac{\tau_{\theta z}(\rho,s)}{\sigma_o} = - \frac{2}{\rho} \{R_e \sum_{n=1}^{\infty} C_n' K_2(\lambda_n \rho t)[\lambda_n \sin \lambda_n s (1 + \lambda_n \tan \lambda_n)$$

$$+ \lambda_n^2 s \cos \lambda_n s]\} - \sum_{k=1}^{\infty} A_k' k\pi [k\pi t K_1(k\pi\rho t)$$

$$+ \frac{2}{\rho} K_2(k\pi\rho t)] \sin k\pi s \quad ,$$

$$\frac{\tau_{\theta\theta}(\rho,s)}{\sigma_o} = R_e \sum_{n=1}^{\infty} C_n' \{-2\nu\lambda_n^2 t K_2(\lambda_n \rho t) \cos \lambda_n s$$

$$- \frac{s}{\rho} \lambda_n \sin \lambda_n s [\lambda_n K_1(\lambda_n \rho t) + \frac{2}{\rho t} K_2(\lambda_n \rho t)]$$

$$- \frac{4}{\rho^2 t} K_2(\lambda_n \rho t) \lambda_n s \sin \lambda_n s + [2-2\nu + \lambda_n \tan \lambda_n]^*$$

$$*[\frac{1}{\rho} \cos \lambda_n s (\lambda_n K_1(\lambda_n \rho t) + \frac{2}{\rho t} K_2(\lambda_n \rho t)) +$$

$$+ \frac{4}{\rho^2 t} K_2(\lambda_n \rho t) \cos \lambda_n s]\}$$

$$+ \sum_{k=1}^{\infty} A_k' \cos k\pi s [\frac{12}{\rho^2 t} K_2(k\pi\rho t) + \frac{4}{\rho} k\pi K_1(k\pi\rho t)] \quad ,$$

$$\frac{\tau_{rr}(\rho,s)}{\sigma_o} = R_e \sum_{n=1}^{\infty} C_n' \{-2\nu\lambda_n^2 t K_2(\lambda_n \rho t) \cos \lambda_n s$$

$$+ [\lambda_n^2 t K_o(\lambda_n \rho t) + \frac{3\lambda_n}{\rho} K_1(\lambda_n \rho t) + \frac{6}{\rho^2 t} K_2(\lambda_n \rho t)]^*$$

$$*[\lambda_n s \sin \lambda_n s - \cos \lambda_n s (2-2\nu + \lambda_n \tan \lambda_n)]\}$$

$$- \sum_{k=1}^{\infty} A_k' \cos k\pi s \left[\frac{12}{\rho^2 t} K_2(k\pi\rho t) + \frac{4}{\rho} k\pi K_1(k\pi\rho t)\right] ,$$

$$\frac{\tau_\theta(\rho,s)}{\sigma_o} = -\frac{2}{\rho}\left[R_e \sum_{n=1}^{\infty} C_n' \left\{\left(\frac{3}{\rho t} K_2(\lambda_n\rho t) + \lambda_n K_1(\lambda_n\rho t)\right)^*\right.\right.$$

$$\left.\left.*[\cos \lambda_n s\ (2-2\nu + \lambda_n \tan \lambda_n) - \lambda_n s \sin \lambda_n s]\right\}\right]$$

$$- \sum_{k=1}^{\infty} A_k' \cos k\pi s \left[2k^2\pi^2 t\, K_o(k\pi\rho t) + \frac{6k\pi}{\rho} K_1(k\pi\rho t)\right.$$

$$\left. + \frac{12}{\rho^2 t} K_2(k\pi\rho t) - k^2\pi^2 t\, K_2(k\pi\rho t)\right] . \qquad (33a\text{-}f)$$

From the characteristic equations it is seen that the problem has zero eigenvalues in $\beta_o = 0$ and $\lambda_o = 0$. Therefore, for completeness some particular solutions must be added to Z_1 and ψ_1 to account for the zero eigenvalues. Let these solutions be of the following form:

$$\psi_1^o(r,z) = f_o(r) + g_o(r)h_o(z) + m_o(z) , \qquad (34)$$

$$Z_1^o(r,z) = f_*(r) + g_*(r)h_*(z) + m_*(z) . \qquad (35)$$

Solutions of the form (34) and (35) satisfying the differential equations (12) and (13) may be expressed as

$$f_o(r) = a_1^o r^2 + a_2^o/r^2 ,$$

$$g_o(r) = c_2^o/r^2 ,$$

$$h_o(z) = d_1^o + d_2^o z + \frac{2b_1^o}{c_2^o} z^2 + \frac{2b_2^o}{3c_2^o} z^3 ,$$

$$m_o(z) = b_1^o + b_2^o z ; \qquad (36a\text{-}d)$$

$$f_*(r) = E_1 + \frac{E_2}{r^2} + E_3 r^2 + E_4 r^4 ,$$

$$g_*(r) = G_2/r^2 \quad ,$$

$$h_*(z) = H_1 + H_2 z + H_3 z^2 + H_4 z^3 + \frac{2F_3}{3G_2} z^4 + \frac{2F_4}{5G_2} z^5 \quad ,$$

$$m_*(z) = F_1 + F_2 z + F_3 z^2 + F_4 z^3 \quad . \tag{37a-d}$$

It may now be shown that imposing the boundary conditions (25), the regularity conditions at $r = \infty$, and the symmetry conditions with respect to the $z = 0$ plane, and requiring that the resulting stress state be non zero, (36) and (37) substituted into (34) and (35) give

$$\psi_1^\circ(r,z) = -3E\left(\frac{z^2}{r^2} + \frac{1}{2}\right) \quad , \tag{38}$$

$$Z_1^\circ(r,z) = E(2-\nu)\frac{z^3}{r^2} + \frac{Fz}{r^2} + \frac{3E}{2}(1-\nu)z \quad , \tag{39}$$

where E and F are arbitrary constants. Defining the dimensionless constants

$$E' = \frac{E}{\sigma_o a^2} \quad , \quad F' = \frac{F}{\sigma_o a^4} \quad , \tag{40}$$

the stress state generated by the functions ψ_1° and Z_1° may be expressed as

$$\frac{\tau_{rr}^\circ(\rho,s)}{\sigma_o} = -\frac{6F'}{\rho^4} + 6E'\left(\frac{1+\nu}{\rho^2} + \frac{3\nu s^2}{\rho^4 t^2}\right) \quad ,$$

$$\frac{\tau_{\theta\theta}^\circ(\rho,s)}{\sigma_o} = \frac{6F'}{\rho^4} - \frac{18E'\nu s^2}{\rho^4 t^2} \quad ,$$

$$\frac{\tau_{r\theta}^\circ(\rho,s)}{\sigma_o} = -\frac{6F'}{\rho^4} + 3E'\left(\frac{1+\nu}{\rho^2} + \frac{6\nu s^2}{\rho^4 t^2}\right) \quad ,$$

$$\tau_{rz}^\circ = \tau_{zz}^\circ = \tau_{\theta z}^\circ = 0 \quad . \tag{41a-f}$$

We now note that the stress expressions given by (33) correspond to nonzero eigenvalues β_n and λ_n, (n=1,2, ...) and the complete solution

for the perturbation problem is obtained by adding (41) to (33). Thus, for the perturbation problem the boundary conditions at r=a given by (4a-c) may be expressed as

$$\tau_{rr}(1,s) + \tau^{\circ}_{rr}(1,s) = -\frac{\sigma_o}{2} \quad ,$$

$$\tau_{r\theta}(1,s) + \tau^{\circ}_{r\theta}(1,s) = \frac{\sigma_o}{2} \quad , \qquad \text{(42a-c)}$$

$$\tau_{rz}(1,s) + \tau^{\circ}_{rz}(1,s) = 0 \quad .$$

Substituting now from (33) and (41) into (42) and expanding both sides of (42a) and (42b) into Fourier series in cos πks and (42c) into sin πks, we obtain the following infinite system of algebraic equations for the unknown constants A_n', C_n', E' and F':

$$c_j A_j' + \mathrm{Re} \sum_{n=1}^{\infty} d_{jn} C_n' = (-1)^{j+1} \frac{72\nu}{t^2\pi^2 j^2} E' \quad , \quad (j=1,2, \ldots) \qquad (43)$$

$$e_j A_j' + \mathrm{Re} \sum_{n=1}^{\infty} f_{jn} C_n' = (-1)^{j+1} \frac{72\nu}{t^2\pi^2 j^2} E' \quad , \quad (j=1,2, \ldots) \qquad (44)$$

$$a_j A_j' + \mathrm{Re} \sum_{n=1}^{\infty} b_{jn} C_n' = 0 \quad , \quad (j=1,2, \ldots) \qquad (45)$$

$$\mathrm{Re} \sum_{n=1}^{\infty} d_{on} C_n' - 12F' + 12E'(1+\nu + \frac{2\nu}{t^2}) = -1 \quad , \qquad (46)$$

$$\mathrm{Re} \sum_{n=1}^{\infty} f_{on} C_n' - 12F' + 6E'(1+\nu + \frac{2\nu}{t^2}) = 1 \quad . \qquad (47)$$

where

$$a_j = -2\pi j K_2(\pi j t) \quad , \quad (j=1,2, \ldots) \quad ,$$

$$b_{jn} = -[\lambda_n t K_1(\lambda t) + 2K_2(\lambda_n t)]\gamma_{jn}(\lambda_n + \lambda_n^2 \tan \lambda_n + \lambda_n^2 \delta_{jn}) \quad ,$$

$$(j,n = 1,2,3, \ldots) \quad ,$$

$$\gamma_{jn} = (-1)^j \left(\frac{\sin \lambda_n}{\lambda_n - j\pi} - \frac{\sin \lambda_n}{\lambda_n + j\pi}\right) \quad , \quad (j,n = 1,2,3, \ldots) \quad ,$$

$$\delta_{jn} = (-1)^{j+1}\left[-\frac{\cos\lambda_n}{\lambda_n - j\pi} + \frac{\sin\lambda_n}{(\lambda_n - j\pi)^2} + \frac{\cos\lambda_n}{\lambda_n + j\pi} - \frac{\sin\lambda_n}{(\lambda_n + j\pi)^2}\right] ,$$

$$(j,n = 1,2, \ldots)$$

$$c_j = -4\pi j K_1(\pi j t) - \frac{12}{t} K_2(\pi j t) \quad , \quad j-1,2, \ldots) \quad ,$$

$$d_{jn} = \varepsilon_{jn}\{-2\nu\lambda_n^2 t K_2(\lambda_n t) - (2-2\nu + \lambda_n \tan\lambda_n)[\frac{6}{t} K_2(\lambda_n t)$$

$$+ 3\lambda_n K_1(\lambda_n t) + \lambda_n^2 t K_o(\lambda_n t)]\}$$

$$+ \lambda_n \phi_{jn}[\frac{6}{t} K_2(\lambda_n t) + 3\lambda_n K_1(\lambda_n t) + \lambda_n^2 t K_o(\lambda_n t)] \quad ,$$

$$(n=1,2, \ldots; \quad j=0,1,2, \ldots) \quad ,$$

$$f_{jn} = -2\{\varepsilon_{jn}(2-2\nu + \lambda_n \tan\lambda_n)[\frac{3}{t} K_2(\lambda_n t) + \lambda_n K_1(\lambda_n t)]$$

$$- \lambda_n \phi_{jn}[\frac{3}{t} K_2(\lambda_n t) + \lambda_n K_1(\lambda_n t)]\} \quad , \quad (n=1,2, ..; j=0,1,2, ..) \quad ,$$

$$\varepsilon_{on} = 2\frac{\sin\lambda_n}{\lambda_n} \quad , \quad (n=1,2, \ldots) \quad ,$$

$$\varepsilon_{jn} = (-1)^j\left(\frac{\sin\lambda_n}{\lambda_n - j\pi} + \frac{\sin\lambda_n}{\lambda_n + j\pi}\right) \quad , \quad (j,n = 1,2, \ldots) \quad ,$$

$$\phi_{on} = -2\frac{\cos\lambda_n}{\lambda_n} + 2\frac{\sin\lambda_n}{\lambda_n^2} \quad , \quad (n=1,2, \ldots) \quad ,$$

$$\phi_{jn} = (-1)^j\left[-\frac{\cos\lambda_n}{\lambda_n - j\pi} + \frac{\sin\lambda_n}{(\lambda_n - j\pi)^2} - \frac{\cos\lambda_n}{\lambda_n + j\pi} + \frac{\sin\lambda_n}{(\lambda_n + j\pi)^2}\right] \quad ,$$

$$(j,n=1,2, \ldots)$$

$$e_j = -2j^2\pi^2 t K_o(\pi j t) - 6j\pi K_1(\pi j t)$$

$$+ K_2(\pi j t)(\pi^2 j^2 t - \frac{12}{t}) \quad , \quad (j=1,2,\ldots) \; . \quad (48)$$

The infinite system (43-47) may be solved by the "method of reduction", that is by truncating the series at the Nth term and by considering only the first N unknowns in A_j' and C_j'. Note that the coefficients A_j', E', and F' are real and C_j' are complex, (j=1,2, ...). Thus, truncated at the Nth term equations (43-47) provide 3N + 2 equations to determine A_1', .. A_N', E', F', and the real and imaginary parts of C_1', .., C_N'. After determining these constants the stress state in the plate containing a stress-free circular hole and subjected to unidirectional tension at $x = \pm\infty$ may be obtained from (5). Note that the stress coefficients τ_{ij}, (i,j=r,θ,z) which appear in (7) are the sum of τ_{ij} and τ_{ij}° given by (33) and (41).

The solution and the results given in this paper are for a particular loading, i.e., $\sigma_{xx} = \sigma_o$ at $x = \pm\infty$. However, it is clear that the method is applicable to any loading condition for which the problem can be reduced to a perturbation problem with the tractions on the hole surface being the only external loads and for which these tractions can be expressed in terms of Fourier series in θ.

3. Results and Discussion

As indicated before, the solution of the problem under consideration is given in [1]. The main reason for reconsidering the problem is therefore to develop a technique which can be used in the formulation of multilayered plate problems by following a somewhat more systematic approach. A secondary purpose of the present study is by taking advantage of the relative improvement in the computational capabilities since the publication of [1], to verify and complement the results given in [1]. Thus, instead of seven roots of the characteristic equation in the first quadrant considered in [1] twenty roots have been calculated and corresponding higher number of terms have been taken into account in solving the related infinite system of algebraic equations (43-47). Even though it is very difficult to prove the regularity of the infinite system (43-47) theoretically, for the relative dimensions considered the convergence seems to be extremely good. Even the results given in [1] which are based on only seven eigenvalues do not significantly differ from those calculated from twenty eigenvalues. The results given in Tables 1-9

complement those presented in [1] in the sense that they contain the investigation of the influence of the Poisson's ratio which appears to be quite significant, the variation of the stress components other than $\sigma_{\theta\theta}$ and σ_{zz} and the variation of the stress components in radial direction. To show the trends of the distribution of various stresses some results are also given in Figures 2-7. It is important to note that in order to conform to the presentation given in [1] the stresses presented in the tables and in the figures are defined by (see (5))

$$\sigma^1_{ij} = \sigma^b_{ij} + \sigma^c_{ij} \quad , \ (i,j = r,\theta,z) \quad , \tag{49}$$

To obtain the complete solution these stresses must be added to the axisymmetric stress state σ^a_{ij} given by (3).

From (43-47) it may be shown that for $\nu=0$

$$A'_j = 0, \quad C'_j = 0, \ (j=1,2, \ldots) \quad , \quad E' = -\frac{1}{3} \ , \ F' = -\frac{1}{4} \quad , \tag{50}$$

which, substituted through (41), (33) and (7) into (5), reduces to the following plane stress solution:

$$\begin{aligned}
\sigma_{rr} &= \frac{\sigma_o}{2}\left(1-\frac{a^2}{r^2}\right) + \frac{\sigma_o}{2}\left(1 + \frac{3a^4}{r^4} - \frac{4a^2}{r^2}\right) \cos 2\theta \quad , \\
\sigma_{\theta\theta} &= \frac{\sigma_o}{2}\left(1 + \frac{a^2}{r^2}\right) - \frac{\sigma_o}{2}\left(1 + \frac{3a^4}{r^4}\right) \cos 2\theta \quad , \\
\sigma_{r\theta} &= -\frac{\sigma_o}{2}\left(1- \frac{3a^4}{r^4} + \frac{2a^2}{r^2}\right) \sin 2\theta \quad , \\
\sigma_{zz} &= \sigma_{rz} = \sigma_{\theta z} = 0 \quad .
\end{aligned} \tag{51a-f}$$

From a practical viewpoint perhaps the most important results are those given in Table 1 and partially displayed in Figures 2 and 3, namely the variation of the hoop stress $\sigma_{\theta\theta}$ on the surface of the circular hole. From (51) it may be observed that the "stress concentration factor" $(\sigma_{\theta\theta})_{max}/\sigma_o$ for the plane problem has a value of 3 and is independent of the Poisson's ratio and the coordinate z. On the other hand Table 1 and

Figures 2 and 3 show that the stress concentration factor may vary with the location z/h, the Poisson's ratio ν, and the radius-to-thickness ratio a/h quite considerably. The stress concentration factor is maximum for z=0 and is greater than the corresponding value for the plane problem. The table and Figure 3 show that $\sigma^1_{\theta\theta}$ at z=0 increases with increasing values of ν, and approaches the plane stress and plane strain values (i.e., $\sigma^1_{\theta\theta} = 2\sigma_o$) as a/h approaches infinity and zero, respectively, becoming a maximum for some value of a/h between 0.5 and 1. For ν=0.5 this maximum may be as much as 15% greater than the corresponding plane stress value.

Table 2 and Figures 4 and 5 show the calculated results for $(-\sigma_{zz}/\sigma_o \cos 2\theta)$. From Table 2 and Figure 4 it may be observed that for a fixed value of ν $(-\sigma_{zz}/\sigma_o \cos 2\theta)$ increases with the decreasing ratio a/h and in limit as $(a/h) \to 0$, away from the plane boundaries $z=\pm h$, it approaches the expected plane strain value of 2ν. Also, for $(a/h) \to \infty$ σ_{zz} approaches zero which is the expected plane stress result. Figure 2 implies that

$$\frac{\partial}{\partial z}\sigma_{zz}(r,\theta,h) = 0 \quad . \tag{52}$$

That this is indeed the case may be seen by considering the third stress equilibrium equation

$$\frac{\partial\sigma_{rz}}{\partial r} + \frac{1}{r}\frac{\partial\sigma_{\theta z}}{\partial\theta} + \frac{\partial\sigma_{zz}}{\partial z} + \frac{\sigma_{rz}}{r} = 0 \tag{53}$$

and by observing that at z=h

$$\sigma_{rz}(r,\theta,h) = 0 \quad , \quad \sigma_{\theta z}(r,\theta,h) = 0 \quad , \tag{54}$$

or

$$\frac{\partial}{\partial r}\sigma_{rz}(r,\theta,h) = 0 \quad , \quad \frac{\partial}{\partial\theta}\sigma_{\theta z}(r,\theta,h) = 0 \quad . \tag{55}$$

Similarly, symmetry considerations require that

$$\frac{\partial}{\partial z}\sigma_{zz}(r,\theta,0) = 0 \quad , \tag{56}$$

which may also be observed form Figure 4. From Figure 5 it may be observed that again as $(a/h) \to \infty$ σ_{zz} approaches zero, the expected plane stress solution, and for $(a/h) \to 0$ $(-\sigma_{zz}/\sigma_o \cos 2\theta) \to 2\nu$ which is the plane strain solution. As ν and a/h vary in the intervals [0.5,0] and $(0,\infty)$ respectively, unlike $\sigma_{\theta\theta}$ the axial stress σ_{zz} varies between the corresponding plane strain and plane stress values.

The distribution of the shear stress $\sigma_{\theta z}$ on the surface of the hole is given in Table 3 and Figure 6. Again, it may be noted that the limiting cases of plane stress and plane strain solutions are recovered as $(a/h) \to \infty$ and $(a/h) \to 0$, $\sigma_{\theta z}$ goes through a maximum in $0.5<(a/h)<1$ and for $(z/h) \cong 0.8$ and increases with increasing ν.

Tables 4-9 show the spatial distribution of the stresses for a=h and ν=0.25. It may be seen that as $r \to \infty$ the stresses given in these tables added to σ^a_{ij} given by (3) approach the homogeneous solution (1). The variation $\sigma^1_{\theta\theta}$ and σ^1_{zz} with r/a is also shown in Figure 7.

The first twenty roots of the characteristic equation (30) are given in Table 10. They seem to agree with the first seven roots calculated by Alblas in nearly all significant digits.

References

1. J.B. Alblas, "Theorie van de Driedimensionale Spanningstoestand in een Doorboorde Plaat", Ph.D. Thesis, H.J. Paris - Amsterdam 1957.

2. R.W. Little, Elasticity, Prentice-Hall, Englewood Cliffs, New Jersey, 1973.

3. E.I. Aguf and V.Z. Vasil'ev, "First Fundamental Problem for a Layer with a Circular Hole", Izv. AN. SSSR Mekhanika Tverdogo Tela. (Mechanics of Solids) Vol. 15, No. 4, pp. 68-77, 1980.

4. E. Sternberg and M.A. Sadowski, "Three-Dimensional Solution for the Stress Concentration Around a Circular Hole in a Plate of Arbitrary Thickness", J. Appl. Mech., Vol. 16, pp 27-38, 1949.

Acknowledgment: This work was supported by NSF under the Grant CME-7809737 and by NASA-Langley under the Grant NGR 39-007-011.

TABLE 1

Distribution of the normalized hoop stress $\frac{-\sigma^1_{\theta\theta}}{\sigma_o \cos 2\theta}$ at the hole boundary r=a.

	z/h \ a/h	0.5	1.0	1.5	2.0	3.0	4.0	5.0
ν=0.15	0.	2.039	2.048	2.041	2.033	2.021	2.014	2.010
	0.25	2.039	2.045	2.037	2.029	2.018	2.012	2.008
	0.50	2.036	2.031	2.022	2.015	2.008	2.005	2.004
	0.75	2.010	1.991	1.987	1.987	1.991	1.994	1.995
	0.90	1.942	1.934	1.947	1.959	1.975	1.983	1.988
	1.0	1.809	1.864	1.904	1.931	1.960	1.975	1.982
ν=0.25	0.	2.082	2.100	2.083	2.064	2.039	2.026	2.018
	0.25	2.082	2.093	2.075	2.057	2.034	2.022	2.015
	0.50	2.077	2.066	2.045	2.032	2.017	2.011	2.007
	0.75	2.028	1.989	1.980	1.980	1.986	1.990	1.992
	0.90	1.901	1.886	1.908	1.929	1.957	1.972	1.980
	1.0	1.665	1.762	1.834	1.881	1.932	1.957	1.970
ν=0.35	0.	2.140	2.167	2.135	2.103	2.062	2.040	2.028
	0.25	2.140	2.156	2.122	2.091	2.054	2.035	2.024
	0.50	2.133	2.112	2.076	2.052	2.028	2.017	2.011
	0.75	2.055	1.991	1.975	1.974	1.980	1.986	1.990
	0.90	1.860	1.834	1.867	1.898	1.939	1.960	1.972
	1.0	1.507	1.651	1.759	1.829	1.903	1.939	1.958
ν=0.50	0.	2.254	2.299	2.235	2.175	2.102	2.065	2.045
	0.25	2.255	2.279	2.212	2.155	2.089	2.056	2.038
	0.50	2.244	2.202	2.135	2.091	2.048	2.029	2.019
	0.75	2.116	2.001	1.970	1.966	1.973	1.981	1.986
	0.90	1.799	1.749	1.799	1.848	1.909	1.941	1.959
	1.0	1.242	1.464	1.635	1.743	1.857	1.910	1.938

TABLE 2

Distribution of the normalized axial stress $-\sigma_{zz}/\sigma_o \cos 2\theta$ at the hole boundary r=a

	z/h \ a/h	0.5	1.0	1.5	2.0	3.0	4.0	5.0
ν=0.15	0.	0.258	0.163	0.102	0.067	0.034	0.020	0.013
	0.25	0.248	0.152	0.094	0.061	0.031	0.018	0.012
	0.50	0.216	0.119	0.070	0.044	0.022	0.013	0.008
	0.75	0.135	0.059	0.031	0.019	0.009	0.005	0.003
	0.90	0.048	0.016	0.007	0.004	0.002	0.001	0.001
	1.0	0.	0.	0.	0.	0.	0.	0.
ν=0.25	0.	0.432	0.268	0.165	0.107	0.054	0.032	0.021
	0.25	0.416	0.250	0.152	0.098	0.049	0.029	0.019
	0.50	0.359	0.195	0.112	0.071	0.035	0.020	0.013
	0.75	0.223	0.096	0.050	0.030	0.014	0.008	0.005
	0.90	0.079	0.026	0.012	0.006	0.003	0.001	0.001
	1.0	0.	0.	0.	0.	0.	0.	0.
ν=0.35	0.	0.613	0.374	0.226	0.145	0.072	0.042	0.028
	0.25	0.589	0.349	0.208	0.133	0.065	0.038	0.025
	0.50	0.507	0.270	0.153	0.096	0.046	0.027	0.017
	0.75	0.312	0.132	0.068	0.040	0.018	0.010	0.006
	0.90	0.109	0.035	0.016	0.008	0.003	0.002	0.001
	1.0	0.	0.	0.	0.	0.	0.	0.
ν=0.50	0.	0.902	0.539	0.317	0.200	0.097	0.056	0.036
	0.25	0.866	0.502	0.291	0.182	0.088	0.051	0.033
	0.50	0.742	0.386	0.214	0.131	0.062	0.035	0.023
	0.75	0.451	0.187	0.094	0.054	0.024	0.013	0.009
	0.90	0.155	0.049	0.021	0.011	0.004	0.002	0.001
	1.0	0.	0.	0.	0.	0.	0.	0.

TABLE 3

Distribution of the normalized shear stress $-\sigma_{\theta z}/\sigma_o \sin 2\theta$ at the hole boundary r=a

	z/h \ a/h	0.5	1.0	1.5	2.0	3.0	4.0	5.0
ν=0.15	0.	0.	0.	0.	0.	0.	0.	0.
	0.25	0.023	0.030	0.024	0.019	0.011	0.007	0.005
	0.50	0.052	0.059	0.046	0.034	0.020	0.013	0.009
	0.75	0.092	0.079	0.057	0.041	0.023	0.014	0.010
	0.90	0.095	0.065	0.043	0.030	0.016	0.010	0.007
	1.0	0.	0.	0.	0.	0.	0.	0.
ν=0.25	0.	0.	0.	0.	0.	0.	0.	0.
	0.25	0.042	0.051	0.041	0.031	0.018	0.012	0.008
	0.50	0.093	0.101	0.077	0.057	0.032	0.021	0.014
	0.75	0.161	0.134	0.094	0.066	0.037	0.023	0.016
	0.90	0.164	0.108	0.071	0.048	0.026	0.016	0.011
	1.0	0.	0.	0.	0.	0.	0.	0.
ν=0.35	0.	0.	0.	0.	0.	0.	0.	0.
	0.25	0.063	0.075	0.058	0.043	0.025	0.016	0.011
	0.50	0.140	0.146	0.109	0.078	0.044	0.028	0.019
	0.75	0.237	0.192	0.131	0.091	0.050	0.031	0.021
	0.90	0.238	0.154	0.098	0.066	0.035	0.021	0.014
	1.0	0.	0.	0.	0.	0.	0.	0.
ν=0.50	0.	0.	0.	0.	0.	0.	0.	0.
	0.25	0.100	0.115	0.086	0.062	0.034	0.021	0.014
	0.50	0.221	0.222	0.159	0.112	0.061	0.038	0.025
	0.75	0.368	0.287	0.190	0.129	0.068	0.041	0.028
	0.90	0.362	0.227	0.141	0.093	0.048	0.029	0.019
	1.0	0.	0.	0.	0.	0.	0.	0.

TABLE 4

Variation of $-\sigma_{zz}/\sigma_o \cos 2\theta$ with r/a, ($a/h = 1$, $\nu = 0.25$)

z/h \ r/a	1.0	1.25	1.5	1.75	2.0	2.5	3.0	4.0	5.0
0.	0.268	0.103	0.032	0.004	-0.005	-0.005	-0.002	0.	0.
0.25	0.250	0.092	0.027	0.003	-0.005	-0.005	-0.002	0.	0.
0.50	0.195	0.062	0.015	0.	-0.004	-0.003	-0.001	0.	0.
0.75	0.096	0.021	0.003	-0.001	-0.002	-0.001	0.	0.	0.
0.90	0.026	0.004	0.	0.	0.	0.	0.	0.	0.
1.0	0.	0.	0.	0.	0.	0.	0.	0.	0.

TABLE 5

Variation of $-\sigma^1_{\theta\theta}/\sigma_o \cos 2\theta$ with $\frac{r}{a}$, ($a/h = 1$, $\nu = 0.25$)

z/h \ r/a	1.0	1.25	1.5	1.75	2.0	2.5	3.0	4.0	5.0
0.	2.100	1.176	0.836	0.686	0.611	0.547	0.523	0.507	0.503
0.25	2.093	1.170	0.831	0.682	0.608	0.545	0.522	0.507	0.503
0.50	2.066	1.146	0.811	0.667	0.598	0.540	0.519	0.506	0.503
0.75	1.989	1.084	0.767	0.637	0.577	0.530	0.515	0.505	0.502
0.90	1.886	1.009	0.721	0.608	0.559	0.523	0.511	0.504	0.501
1.0	1.762	0.933	0.678	0.584	0.544	0.517	0.508	0.503	0.501

TABLE 6

Variation of $\sigma^1_{rr}/\sigma_o \cos 2\theta$ with r/a , ($^a/_h$ = 1 , ν = 0.25)

z/h \ r/a	1.0	1.25	1.5	1.75	2.0	2.5	3.0	4.0	5.0
0.	0.	-0.178	-0.104	0.001	0.093	0.222	0.301	0.383	0.424
0.25	0.	-0.176	-0.101	0.003	0.094	0.222	0.300	0.383	0.423
0.50	0.	-0.170	-0.093	0.009	0.098	0.222	0.299	0.382	0.423
0.75	0.	-0.158	-0.082	0.015	0.099	0.219	0.296	0.381	0.423
0.90	0.	-0.149	-0.080	0.013	0.094	0.214	0.292	0.379	0.422
1.0	0.	-0.147	-0.085	0.005	0.087	0.209	0.289	0.378	0.422

TABLE 7

Variation of $\sigma_{r\theta}/\sigma_o \sin 2\theta$ with r/a , ($^a/_h$ = 1 , ν = 0.25)

z/h \ r/a	1.0	1.25	1.5	1.75	2.0	2.5	3.0	4.0	5.0
0.	0.	-0.519	-0.637	-0.654	-0.645	-0.613	-0.587	-0.555	-0.537
0.25	0.	-0.519	-0.638	-0.655	-0.646	-0.615	-0.588	-0.555	-0.537
0.50	0.	-0.518	-0.641	-0.660	-0.651	-0.619	-0.591	-0.556	-0.537
0.75	0.	-0.531	-0.658	-0.676	-0.664	-0.626	-0.595	-0.557	-0.538
0.90	0.	-0.563	-0.685	-0.696	-0.678	-0.633	-0.599	-0.558	-0.538
1.0	0.	-0.610	-0.716	-0.716	-0.691	-0.639	-0.602	-0.559	-0.539

TABLE 8

Variation of $-\sigma_{rz}/\sigma_o \cos 2\theta$ with r/a, ($a/h = 1$, $\nu = 0.25$)

z/h \ r/a	1.0	1.25	1.5	1.75	2.0	2.5	3.0	4.0	5.0
0.	0.	0.	0.	0.	0.	0.	0.	0.	0.
0.25	0.	0.011	0.014	0.012	0.009	0.004	0.001	0.	0.
0.50	0.	0.022	0.026	0.021	0.015	0.006	0.002	0.	0.
0.75	0.	0.029	0.028	0.020	0.013	0.005	0.001	0.	0.
0.90	0.	0.021	0.017	0.011	0.007	0.002	0.001	0.	0.
1.0	0.	0.	0.	0.	0.	0.	0.	0.	0.

TABLE 9

Variation of $-\sigma_{\theta z}/\sigma_o \sin 2\theta$ with r/a, ($a/h = 1$, $\nu = 0.25$)

z/h \ r/a	1.0	1.25	1.5	1.75	2.0	2.5	3.0	4.0	5.0
0.	0.	0.	0.	0.	0.	0.	0.	0.	0.
0.25	0.051	0.033	0.019	0.010	0.006	0.001	0.	0.	0.
0.50	0.101	0.058	0.032	0.017	0.009	0.002	0.	0.	0.
0.75	0.134	0.059	0.028	0.014	0.007	0.002	0.	0.	0.
0.90	0.108	0.033	0.015	0.007	0.003	0.001	0.	0.	0.
1.0	0.	0.	0.	0.	0.	0.	0.	0.	0.

TABLE 10

The first 20 roots of the characteristic equation $2\lambda_n + \sin 2\lambda_n = 0$

n	Re (λ_n)	Im (λ_n)
1	2.106196115	1.124364306
2	5.356268699	1.551574373
3	8.536682427	1.775543674
4	11.69917761	1.929404497
5	14.85405991	2.046852462
6	18.00493301	2.141890794
7	21.15341336	2.221722915
8	24.30034206	2.290552287
9	27.44620289	2.351048230
10	30.59129510	2.405012569
11	33.73581432	2.453719208
12	36.87989417	2.498102205
13	40.02362922	2.538866866
14	43.16708835	2.576558851
15	46.31032301	2.611608995
16	49.45337245	2.644363429
17	52.59626714	2.675104424
18	55.73903115	2.704065198
19	58.88168372	2.731440658
20	62.02424045	2.757395360

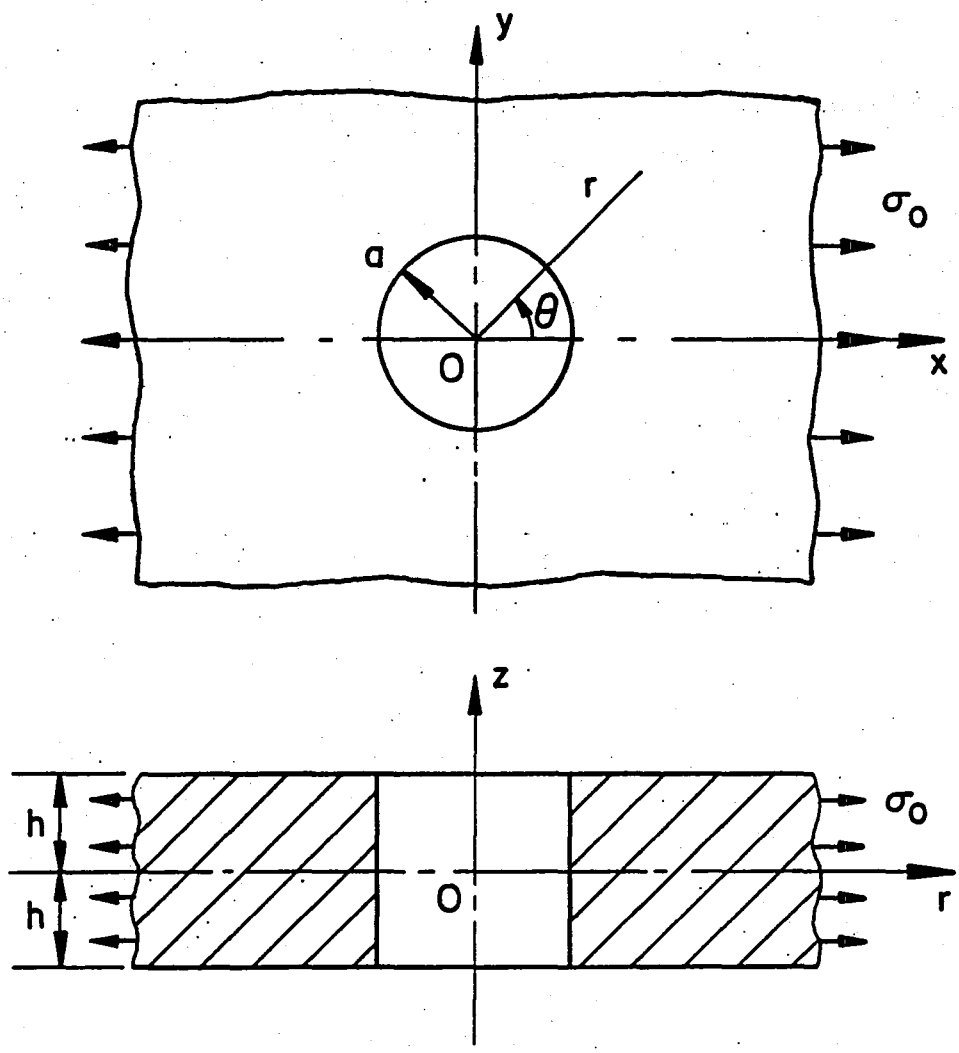

Figure 1. Geometry of a thick plate containing a circular hole.

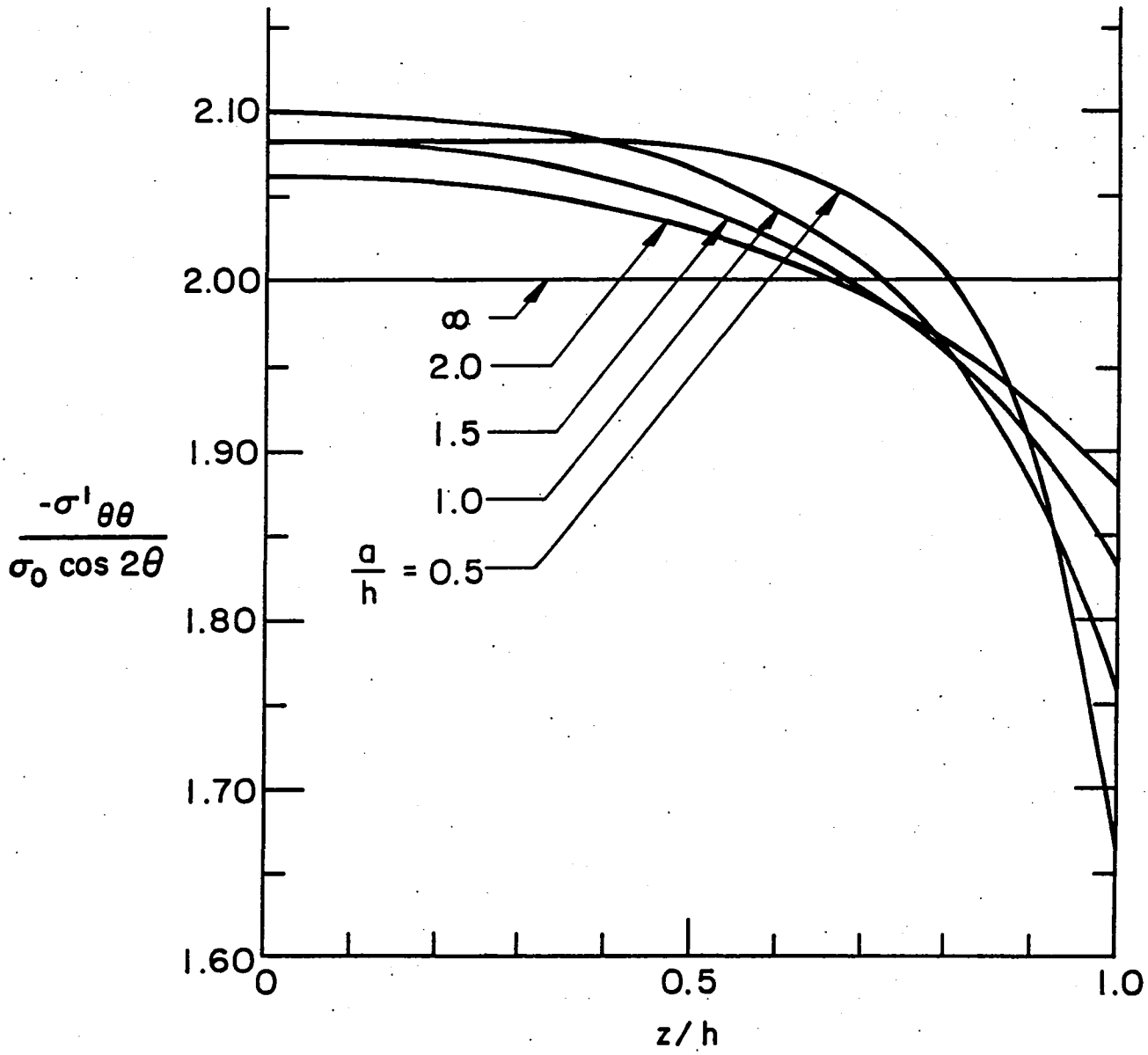

Figure 2. Thickness distribution of the normalized hoop stress $-\sigma^1_{\theta\theta}/\sigma_o \cos 2\theta$ at hole boundary r = a for ν = 0.25 and for various values of a/h.

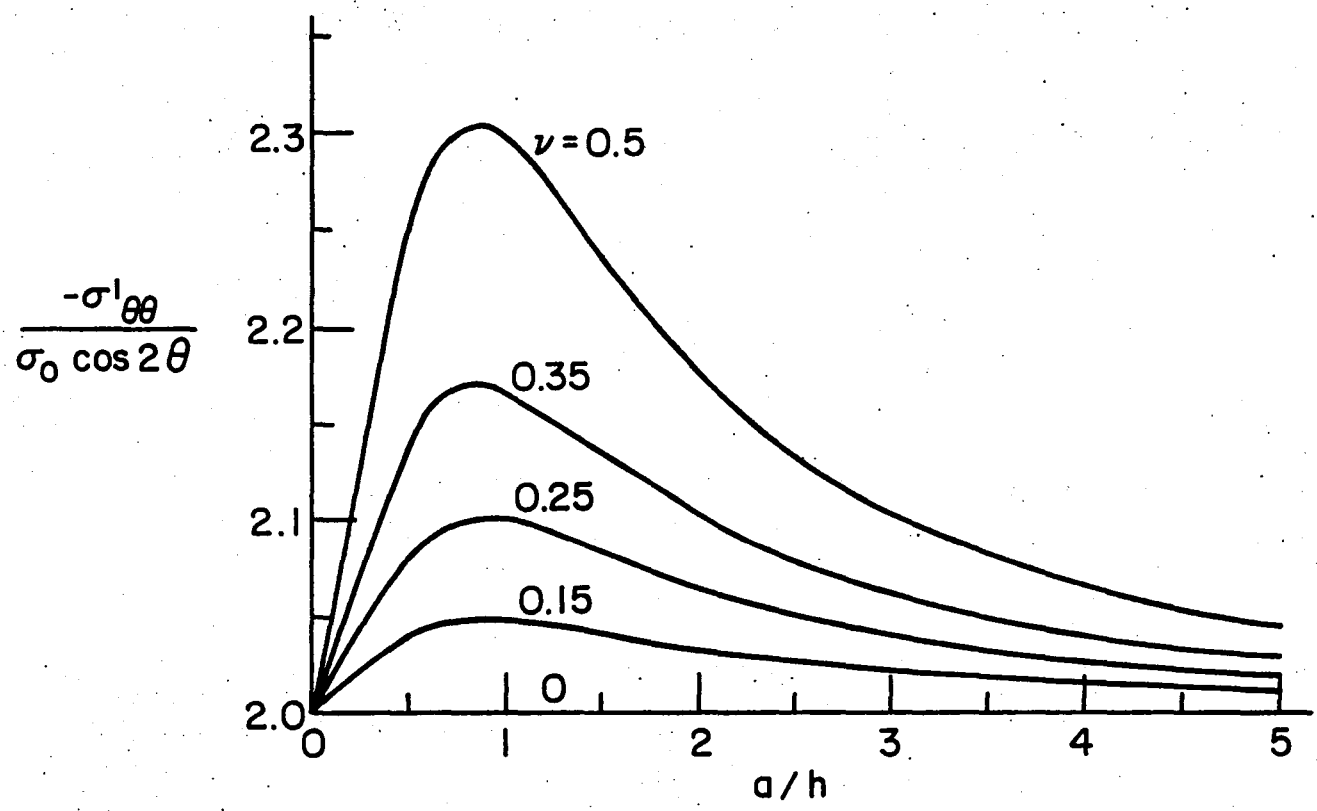

Figure 3. Variation of the normalized hoop stress wiht a/h calculated at z = 0, r = a.

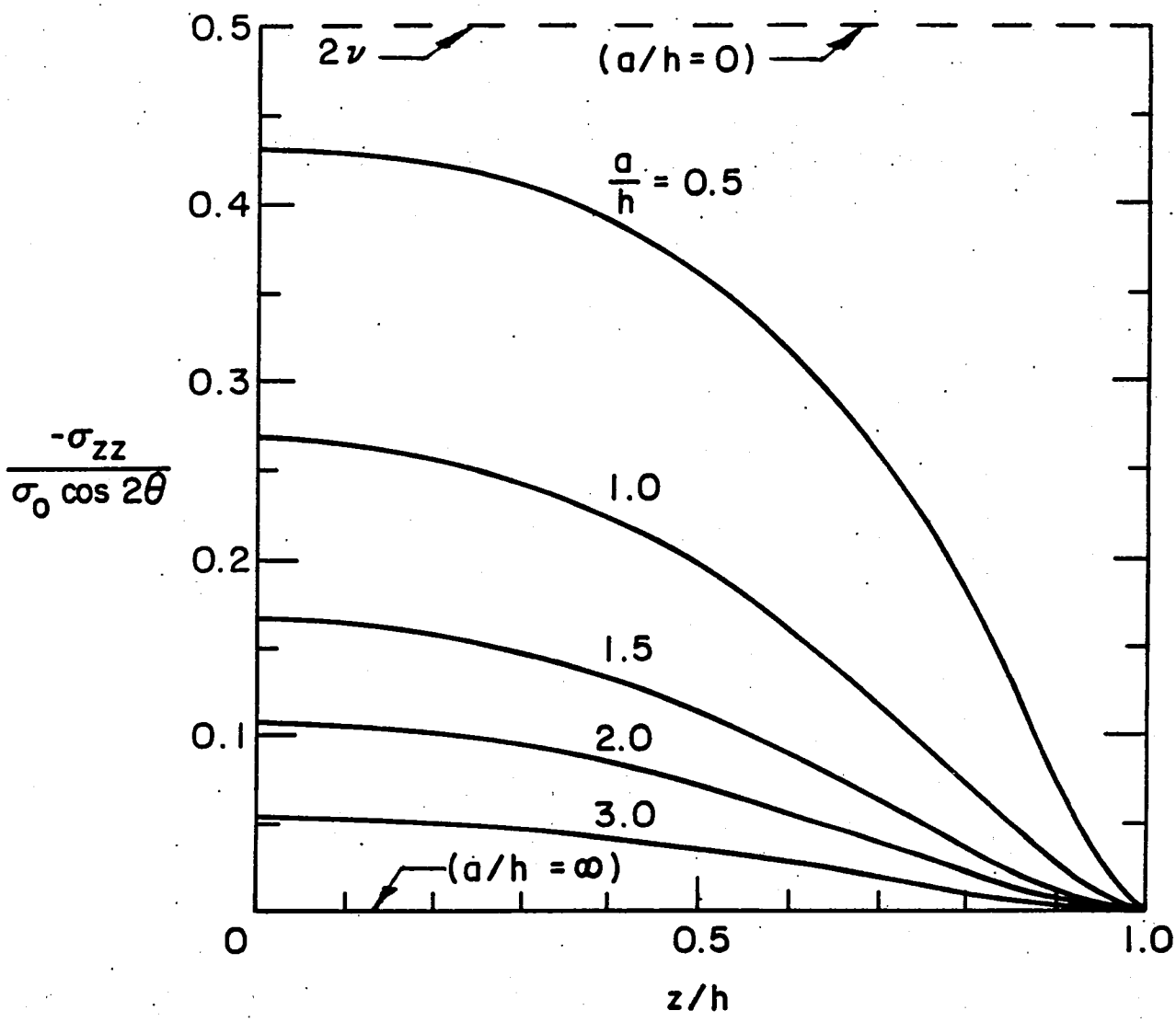

Figure 4. Thickness distribution of the normalized axial stress $-\sigma_{zz}/\sigma_o \cos 2\theta$ at the hole boundary $r = a$ for $\nu = 0.25$ and various values of a/h.

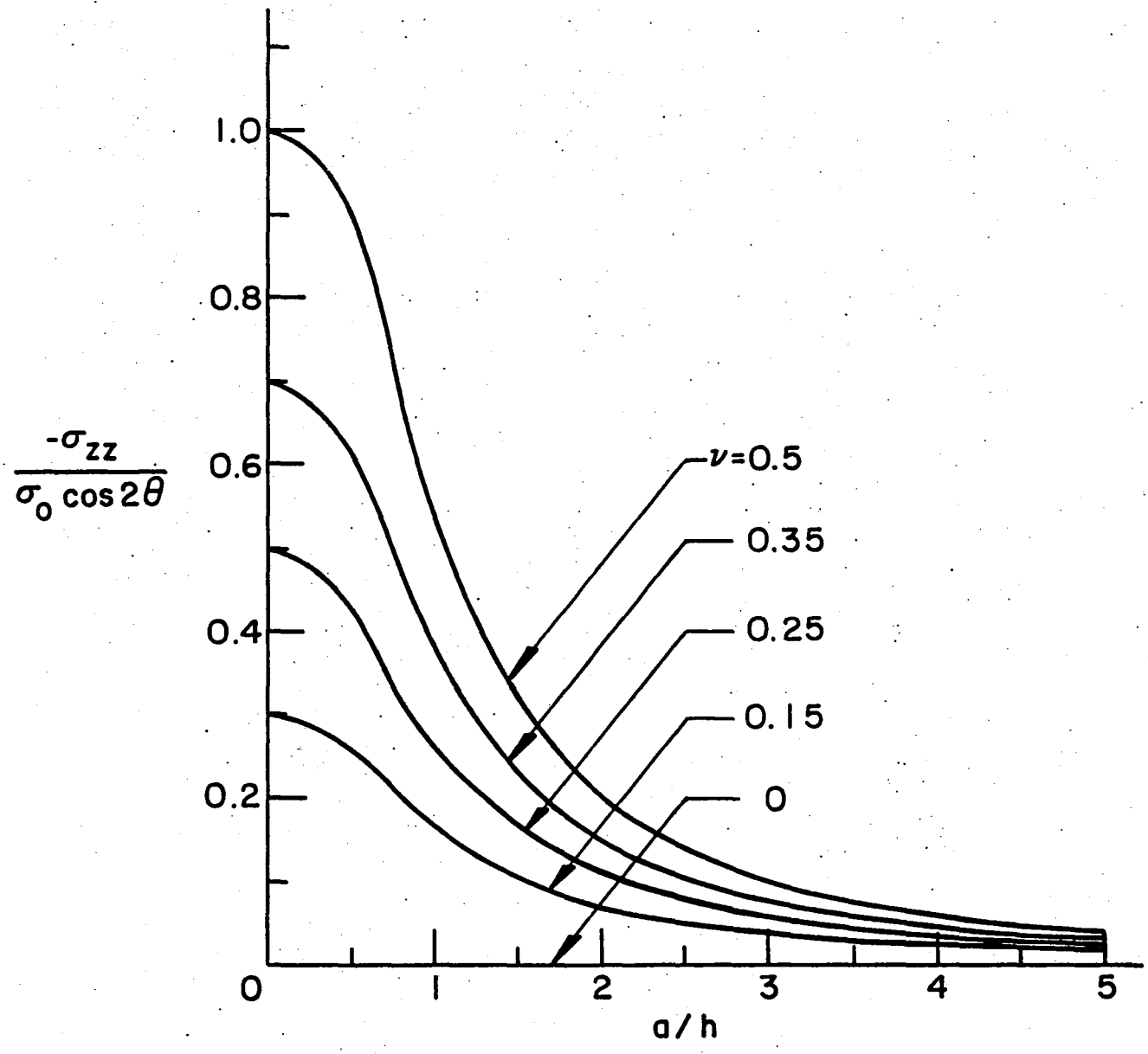

Figure 5. Variation of the normalized axial stress with a/h calculated at z = 0 and r = a.

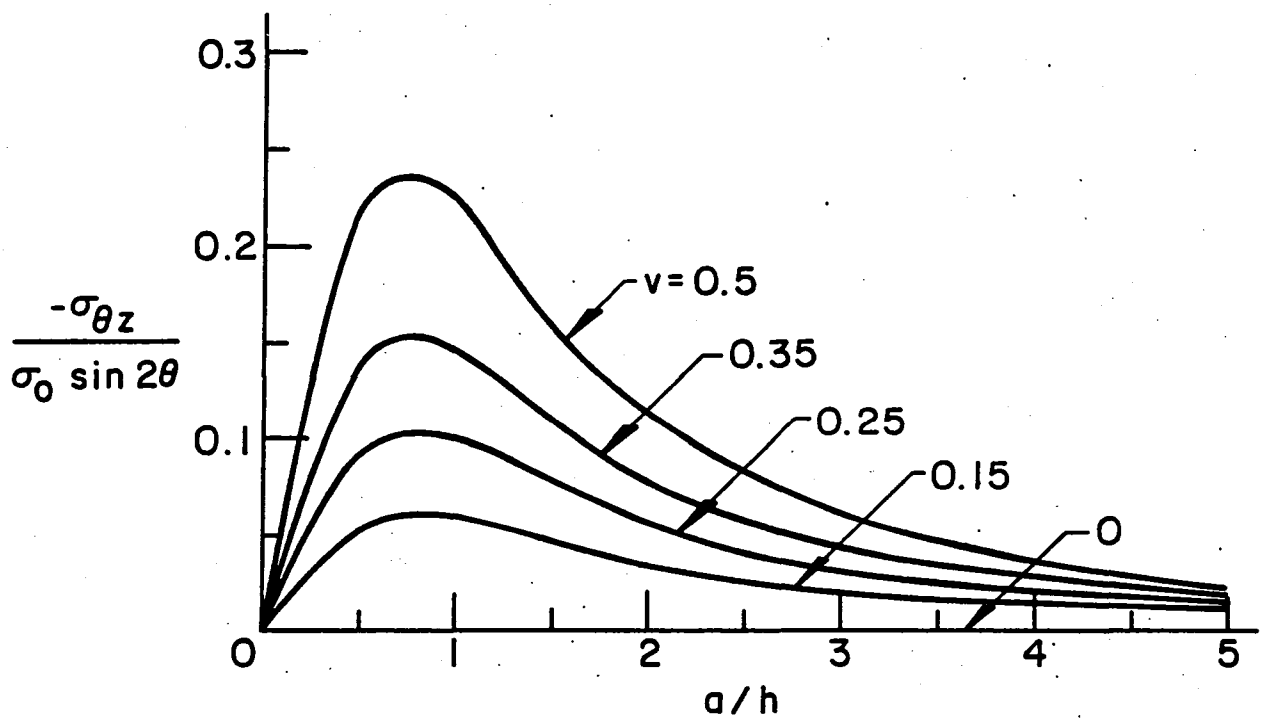

Figure 6. Variation of the normalized shear stress $-\sigma_{\theta z}/\sigma_o \sin 2\theta$ with a/h calculated at r = a and z = h/2.

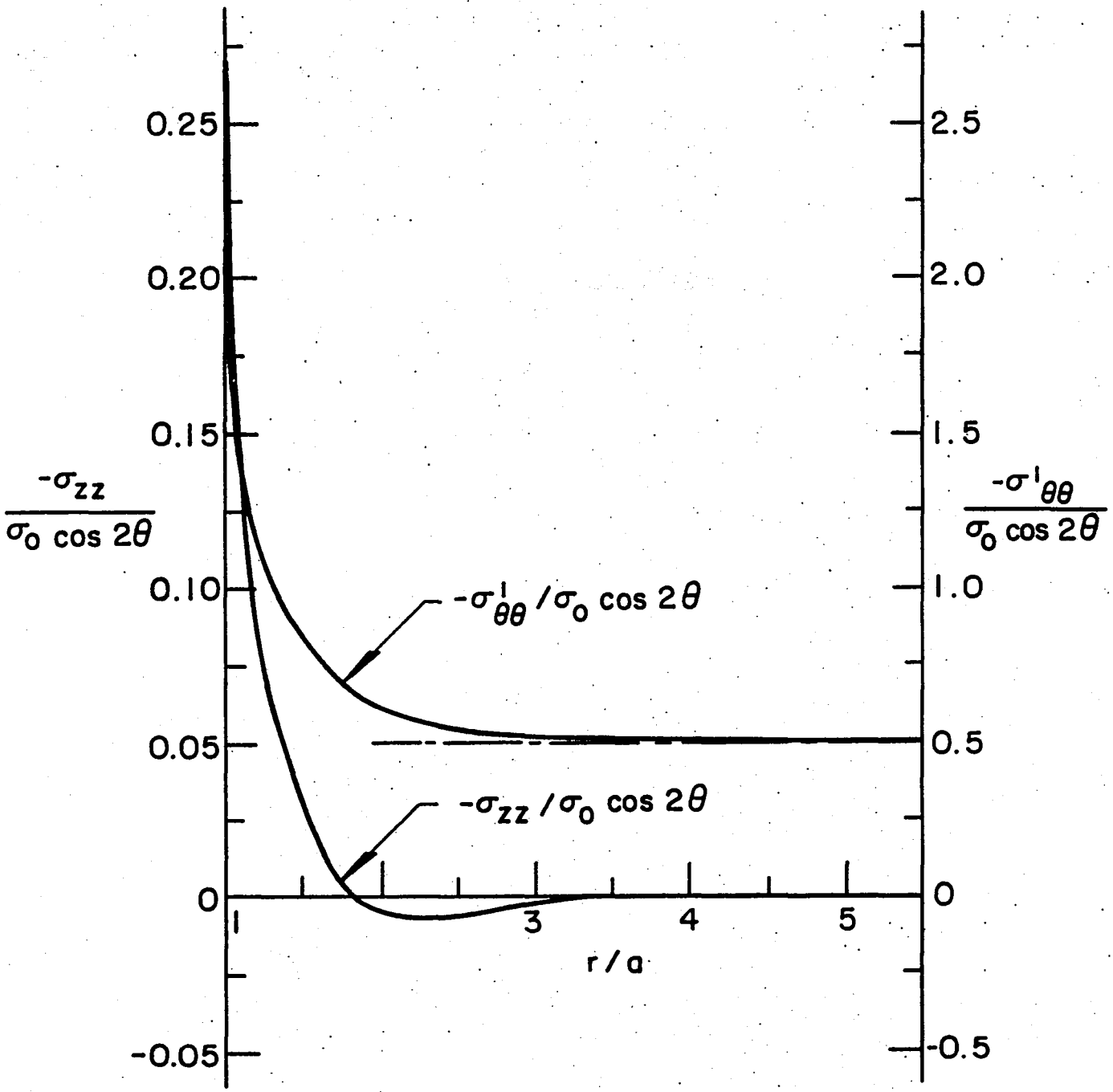

Figure 7. Radial distribution of normalized hoop and axial stresses calculated at z = 0 plane for $\nu = 0.25$ and a = h.

1. Report No.	2. Government Accession No.	3. Recipient's Catalog No.
NASA CR-165986		

4. Title and Subtitle	5. Report Date
THREE-DIMENSIONAL ELASTICITY SOLUTION OF AN INFINITE PLATE WITH A CIRCULAR HOLE	September 1982
	6. Performing Organization Code
7. Author(s)	8. Performing Organization Report No.
F. Delale and F. Erdogan	
9. Performing Organization Name and Address	10. Work Unit No.
Lehigh University Bethlehem, PA 18015	11. Contract or Grant No. NGR 39-007-011
12. Sponsoring Agency Name and Address	13. Type of Report and Period Covered
National Aeronautics and Space Administration Washington, DC 20546	Contractor Report
	14. Sponsoring Agency Code

15. Supplementary Notes

Langley technical monitor: Dr. John H. Crews, Jr.

16. Abstract

In this paper, the elasticity problem for a thick plate with a circular hole is formulated in a systematic fashion by using the z-component of the Galerkin vector and that of Muki's harmonic vector function. The problem was originally solved by Alblas. The reasons for reconsidering it are to develop a technique which may be used in solving the elasticity problem for a multilayered plate and to verify and extend the results given by Alblas. As in the Alblas solution, the problem is reduced to an infinite system of algebraic equations which is solved by the method of reduction. Various stress components are tabulated as functions of a/h, z/h, r/a, and ν, a and $2h$ being the radius of the hole and the plate thickness and ν the Poisson's ratio. Among the additional results of particular interest one may mention the significant effect of the Poisson's ratio on the behavior and the magnitude of the stresses.

17. Key Words (Suggested by Author(s))	18. Distribution Statement
Thick plate Circular hole Unidirectional loading Elasticity Three-dimension stresses	Unclassified - Unlimited Subject Category 39

19. Security Classif. (of this report)	20. Security Classif. (of this page)	21. No. of Pages	22. Price*
Unclassified	Unclassified	32	A03

* For sale by the National Technical Information Service, Springfield, Virginia 22161

End of Document